IEEE Open Access Journal of
Power and Energy

Received 6 March 2020; revised 20 May 2020 and 12 August 2020; accepted 3 October 2020. Date of publication 6 October 2020; date of current version 9 November 2020.

Digital Object Identifier 10.1109/OAJPE.2020.3029118

Technical and Economic Impact of the Inertia Constraints on Power Plant Unit Commitment

CARMELO MOSCA[1] (Member, IEEE), ETTORE BOMPARD[1] (Member, IEEE), GIANFRANCO CHICCO[1] (Fellow, IEEE), BENEDETTO ALUISIO[2] (Member, IEEE), MICHELA MIGLIORI[2] (Student Member, IEEE), CHIARA VERGINE[2], AND PAOLO CUCCIA[3]

[1]Dipartimento Energia Galileo Ferraris, Politecnico di Torino, 10129 Turin, Italy
[2]Grid Planning and Interconnection Department, Terna S.p.A., 00156 Rome, Italy
[3]Dispatching Department, Terna Rete Italia S.p.A., 10154 Torino, Italy

CORRESPONDING AUTHOR: G. CHICCO (gianfranco.chicco@polito.it)

ABSTRACT The whole interconnected European network is involved in the energy transition towards power systems based on renewable power electronics interfaced generation. In this context, the major concerns for both network planning and operation are the inertia reduction and the frequency control due to the progressive decommissioning of thermal power plants with synchronous generators. This paper investigates the impact of different frequency control constraints on the unit commitment of power plants resulting from market simulations. The market outputs are compared in terms of system costs, and of frequency stability performance evaluated on the basis of the rate of change of frequency and the maximum frequency excursion. The best compromise solution is found using a multiple-criteria decision analysis method, depending on the choice of the decision maker's weighting factors. The proposed approach is tested on a real case taken from one of the most relevant future scenarios of the Italian transmission system operator. The results show how the best compromise solution that can be found depends on the decision maker preference towards cost-based or frequency stability-based criteria.

INDEX TERMS Frequency stability, inertia constraints, multiple-criteria decision analysis, power system inertia, rate of change of frequency, unit commitment.

NOMENCLATURE

Acronyms

DG	Distributed Generation
ENTSO-E	European Network of Transmission System Operators for Electricity
HVDC	High Voltage Direct Current
MCDA	Multiple-Criteria Decision Analysis
PEIG	Power Electronics Interfaced Generation
RES	Renewable Energy Sources
ROCOF	Rate Of Change Of Frequency
SEW	Socio-Economic Welfare
SNSP	System Non-Synchronous Penetration
TOPSIS	Technique for Order Performance by Similarity to Ideal Solution
TSO	Transmission System Operator

Symbols

c_m	relative closeness coefficient of alternative m to the ideal solution
$(df/dt)_{\max}$	maximum admissible *ROCOF*
f_0	nominal frequency
$f_a(P_a)$	hourly cost curve of the equivalent thermal unit as a function of the injected power P_a
k	information entropy coefficient
m	index of TOPSIS alternatives
p_m	probability for the m-th alternative
r	normalised decision matrix entry for TOPSIS
s	sensitivity matrix coefficients of DC load-flow
u	multi-objective optimization problem solution
v	weighted normalised decision matrix entry
w	aggregated weight entry of the decision matrix
x	binary variable that represents the i-th generator status (0 = offline, 1 = online) at time t

z	index of TOPSIS criterion
A	number of interconnected areas
$E_{k,\min}$	minimum kinetic energy
$E_{k,\mathrm{sys}}$	kinetic energy of the system
F	overall fuel cost
H_i	inertia constant of the i-th generator
H_{sys}	aggregated inertia of the system
J	number of interconnecting lines
M	number of alternatives for TOPSIS
N	total number of thermal power plants
P_{demand}	power demand
P_{export}	exported power through HVDC
P_{import}	imported power through HVDC
P_{PEIG}	power generation by PEIG
$ROCOF_{95\%}$	*ROCOF* occurring in 95% of the cases with violations
S_{ni}	rated power of the i-th generator
S_{tot}	total rated power of the generators
$S_{t,\min}$	minimum available synchronous capacity at hour t
$S_{t,\mathrm{load}}$	demand capacity at hour t
T	transfer capacity constraints of each interconnecting line
Z	number of criteria for TOPSIS
α	coefficient of variation for the groups of performance criteria
δ_m^+, δ_m^-	distance s from the ideal positive and ideal negative solutions for alternative m
$\xi_{\max}$	maximum *SNSP* ratio
ξ_{SNSP}	*SNSP* ratio
λ_z	decision maker's weighting factor
χ_{CO_2}	ratio between the cost of CO_2 calculated in the constrained alternative and in the base case
χ_{fuel}	ratio between the cost of fuel calculated in the constrained alternative and in the base case
χ_{SEW}	ratio between the *SEW* calculated in the constrained alternative and in the base case
ψ	fraction of the demand capacity for $S_{t,\min}$
σ_c	cardinality of the cost-based performance criteria
σ_f	cardinality of the frequency stability performance criteria
E	Shannon entropy
Δ_z	information entropy for criterion z
$\Delta f_{\mathrm{nadir}}$	maximum transient frequency deviation
$\Delta f_{\mathrm{nadir95\%}}$	difference between the nominal frequency and the value of frequency nadir occurring in 95% of the cases with violations
ΔP_{L}	generation load imbalance
$\boldsymbol{a}^+, \boldsymbol{a}^-$	positive and negative ideal solutions
$\mathbf{D}$	matrix of alternatives for each criterion
$\mathbf{R}$	normalised decision matrix
$\mathbf{V}$	weighted normalised decision matrix
$\mathbf{W}$	diagonal weight matrix

I. INTRODUCTION

In 2014 the European countries agreed on the renewable energy target of providing at least 27% of their final energy consumption from renewable energy sources (RES), by 2030, as dictated by the European Union's energy and climate goals for 2030. In 2016 the European Commission proposed a revised Renewable Energy directive [1]. Finally, in 2018 a renewable energy target of 32% for European Union by 2030 has been defined in [2]. As a part of the current European Union climate and energy strategy, the Italian power system is involved in this energy transition: in the European context, the planning scenario "Distributed Generation" ("DG") [3], forecasts a significant increase in renewable installed generation capacity, mainly in the South of Italy and in the main Islands. Since RES are implementing power electronic converters in their interconnecting interface (Power Electronics Interfaced Generation – PEIG), they are interpreted as non-synchronous generation [4]. The increasing share of "inverter-based" generation sources that substitute the synchronous units (today responsible for the main part of the system inertia), together with the increasing power electronic loads in the power systems, lead to the reduction of the overall system inertia [5] with the following main operational implications after disturbances: higher frequency oscillations, reduction in lower values of the frequency (named "nadir"); increase in higher value of the frequency (named "zenith"), higher Rates of Change of Frequency (named "*ROCOF*"). Traditionally, low levels of synchronous inertia have been a concern for smaller, isolated systems. Nevertheless, today utilities and regulations are recognizing this issue also in larger power systems, investigating possible effects and countermeasures.

Some studies have proposed market designs that incorporate primary frequency response in the ancillary service markets [6], taking into account the provision of inertia and the effects of uncertainties from RES [7]. Moreover, the determination of the minimum commitment cost for providing inertia services from fast-responding storage devices has been addressed in [8].

In the European context, the system protection and dynamics sub-group of the European Network Transmission System Operator (ENTSO-E) detected the impact of the decreased system inertia in the continental Europe power systems in case of the reference incident and system split. The "reference incident" is the basis for the frequency containment reserve calculations and protection scheme settings, according to ENTSO-E, and it changes according to the size of the system [9]. The main challenge is related to the identification of a minimum allowable penetration level of synchronous generation in the system [10]. This limit has effective implications both on the renewable energy and economic targets, as it can result in renewable energy sources curtailment, or extra

TABLE 1. Comparisons among relevant references.

Paper	Inertia constraints	Costs	Decision-making method	Case study	Dynamic simulations
this paper	1. Minimum kinetic energy based on a sensitivity analysis on the worst contingency. 2. Minimum available synchronous capacity. 3. Maximum level of *SNSP*.	Economic outcomes from market simulations evaluated in terms of *SEW*, cost of CO_2 emissions, and cost of fuel.	A multiple-criteria decision analysis (TOPSIS method) is implemented.	Yearly 2030 scenarios from the Italian TSO, hourly resolution.	Hourly dynamic simulations performed with an aggregate model calibrated on real events and developed in [30] to evaluate the results from unit commitment.
[10]	1. Minimum kinetic energy based on the worst contingency. 2. Frequency deviation limit	Minimize expected costs for generation, frequency ancillary services, inertia provision by synchronous compensators and wind reserve.	No method implemented.	Australian National Energy Market, one-day scenario, 5-min dispatch.	Dynamic simulations performed for every economic dispatch with a single bus model.
[11]	1. Minimum kinetic energy based on the worst contingency. 2. Minimum kinetic energy based on the worst contingency each time step	Minimize expected costs for operation and reserve, including variable operation and maintenance, carbon and fuel, and start-up cost. No minimum run time considered.	No method implemented.	Ireland and North Ireland power system, two study years (2012 and 2020), hourly dispatch.	No dynamic simulations performed. *ROCOF* calculated using the swing equation.
[12]	1. *ROCOF* limit 2. Steady state frequency 3. Nadir limit	System costs are not the main focus of the paper.	No method implemented.	Australian National Energy Market, different scenarios (low and high demand, various levels of variable generation). Fixed and variable contingencies. No real generation units.	No dynamic simulations performed.
[15]	1. *ROCOF* limit 2. Steady state frequency 3. Nadir limit	Minimize system operation costs (generation, interconnection, RES curtailment costs).	No method implemented.	Great Britain power system, 20 different scenarios by RES and demand, inspired to the TSO. No real generation units.	No dynamic simulations performed.
[17]	1. *ROCOF* limit 2. Nadir limit	Minimize system operation costs, focus on the economic value of inertia for a possible inertia market.	No method implemented.	Variable scenarios under different generation mix and wind penetration. No real case studies.	No dynamic simulations performed.

costs for running conventional synchronous plants. Different studies have investigated unit commitment and economic dispatch-based strategies, using constraints and operational metric formulations related to the initial *ROCOF* following an imbalance and the level of wind curtailment [11]. Some works present novel mixed integer linear dispatch models that describe frequency performance requirements as a function of both system inertia and maximum contingency size, to reduce operational costs and renewable curtailment [12], to optimize energy production and the allocation of inertial and primary frequency response, as well as enhanced frequency response,[1] against the largest plant outage [15], to apply stochastic unit commitment to schedule multiple frequency services [16], or to quantify the economic value of inertia [17]. In [18] the unit commitment is updated by exploiting more conventional generation when the nadir for the worst contingency is too low. The environmental-economic generation dispatch while considering frequency stability in the optimization problem has been considered in [19], leaving in any case the final decision to the Transmission System Operator (TSO). Various methods have been proposed in the literature to solve problems with conflicting objectives to find the best compromise, as in the case of environmental, economic or security targets [20]. In some cases, the multi-objective is converted into a single-objective optimization problem by weighted aggregation method. Nevertheless, multi-objective evolutionary algorithms have shown the ability of finding effective optimal solutions [21]. Other works implemented the constraints by linearizing the inertia constraint [22]–[24], even if the real behaviour is strictly non-linear. However, ensuring very conservative results that would lead to costs overestimation make these approaches not easy to be exploited for real planning studies by the TSO. Furthermore, a practical methodology to select the best compromise solution in the inertia-dependent unit commitment is still needed. Table 1 summarises the characteristics of some relevant references indicated above, comparing them with the present work.

This paper investigates the impact of different frequency control constraints on the unit commitment of power plants, proposing a methodology to apply in the conventional economic dispatch algorithm currently used by the power system utilities.

A systematic market analysis is carried out through consecutive steps considering different significant ''inertia

[1] Enhanced frequency response was introduced in recent years in Great Britain [13], where further reform is now in progress [14].

thresholds": the outputs are compared in terms of overall system costs and frequency security performance, using dynamic simulations. A methodology to find the best compromise in a technical-economic view is outlined, using a multiple criteria decision analysis methodology.

The approach is tested on the small insular power system of the Sardinia Island using the results of market simulations in the DG 2030 scenario, characterized by the most relevant renewable energy penetration. The DG 2030 scenario comes from the Ten Years Network Development Plan (TYNDP) 2018 of ENTSO-E deployed by the Italian TSO [3].

The main contribution of this paper is the implementation of frequency security constraints in the TSO's economic dispatch model, with the possibility to select different constraints to optimize the unit dispatching. In the second stage, the Technique for Order Performance by Similarity to Ideal Solution (TOPSIS) method has been applied to help the decision maker to extract the best compromise solution, in terms of frequency performance and economic costs.

The paper is organized as follows. Section II illustrates the problem formulation and market analysis. Section III presents the proposed methodology. Section IV contains the case study and the simulation results. Section V concludes the paper.

II. MARKET ANALYSIS CONSIDERING INERTIA CONSTRAINTS

A. UNIT COMMITMENT PROBLEM FORMULATION

The problem of the minimum cost constrained dispatch is assuming an increasing relevance in planning studies, since new constraints are imposed to optimum dispatch of hydro-thermal generation system by growing variable RES production, not uniformly distributed in some geographical areas of the country. To face the new situation while saving both economy and security of operation, new methodologies and algorithms were developed and implemented in the computing tools of the Italian TSO. In general, the unit commitment problem has to be solved finding the set of powers generated by the thermal units, minimizing the overall fuel cost and respecting the upper and lower capacity bounds of both thermal units and interconnection lines [25]. Normally, the solution of the problem for an interconnected power system has to consider a set of different factors, such as global interchange constraints between contiguous areas, depending on the capability of the interconnecting lines and on possible contractual agreements, and local constraints relevant to the carrying capability of each individual interconnection.

In this paper, additional constraints related to the frequency stability and security are considered and implemented in the market simulations. Promed Grid is the market simulator used by the Italian TSO to perform the optimization procedure of the generation power plants emulating a coordinated hydro-thermal generation scheduling optimization over a year with hourly details [26]. The aim is the minimization of the overall generation cost to maximize the market surplus, defined as the sum of the producer surplus, consumer surplus and congestion rents. This allows the TSO to assess the economic social welfare gain related to the development actions in planning scenarios characterized by the generation portfolio evolution towards the inverter-based type, consistently with the basic approaches indicated by ENTSO-E [27]. The simulations are based on the market zones equivalent network model, with the entire European interconnected system as the perimeter of the study. The merit order of the offers is created on the basis of the generation variable costs, the bidding strategies of the units, the main constraints of thermal units such as flexibility, technology, and provision of reserve, and the optimization of the usage of water reservoir of the hydro power plants and renewable generation. The simulation of the market behaviour is obtained by calculating the optimal medium-term operation schedule of the power system. To determine the market outcomes, the solution of a large quadratic programming optimization problem is performed, which minimizes the overall cost borne in one year by the energy buyers, based on the assumptions on the producers bidding behaviour at different operation points. This approach is rigorous and, most importantly, fast, as well as robust and conceptually simple, as shown in [28]. An equivalent network model of the interconnected European power system is used. The European market zones are represented as single nodes equipped with detailed generation and load information and interconnected by means of single branches of transmission capacity equal to the real one (the hourly power transfer capacity in each direction is detailed to adequately model real daily and seasonal differences). Electricity price forecasting is performed through two computational steps:

① *Unit Commitment*: the hourly on/off state of each thermal unit on the basis of a merit order of the offers and fulfilling the constraints of the electric system is determined.

② *Dispatching:* the hourly production scheduling of each thermal unit is determined in coordination with the hydro dispatching, compliant with the electric system constraints.

Let us consider a multi-area system with A areas interconnected by J lines. For each area $a = 1,\ldots,A$, let us denote as $f_a(P_a)$ the hourly cost curve of the equivalent thermal unit in function of the power P_a to be supplied. The multi-area thermal dispatching problem is formulated with the objective is to find the power P_a that minimizes the overall fuel cost F subject to the minimum T_{jm} and the maximum T_{jM} transfer capacity constraints of each interconnecting line $j = 1,\ldots,J$. Let us further denote with s_{jn} the sensitivity matrix coefficients of the DC load-flow. The power transfer on line $j = 1,\ldots,J$ is expressed as:

$$T_j = \sum\nolimits_{a=1}^{A} s_{ja} P_a \tag{1}$$

The optimal multi-area thermal dispatching is expressed as:

$$\min F = \sum\nolimits_{a=1}^{A} f_a(P_a) \tag{2}$$

subject to:

$$\sum_{a=1}^{A} P_a = 0 \tag{3}$$

$$T_j - T_{jm} \geq 0;\ T_{jM} - T_j \geq 0 \text{ for } j = 1, \ldots, J \tag{4}$$

The market simulator solves the hydro-thermal dispatching optimization problem considering flexibility constraints (duration of permanence in the same ON/OFF state) for thermal generation units, and zonal reserve margin constraints.

B. INERTIA CONSTRAINTS

The dynamic behaviour of a synchronous generation unit in a power system is determined by the swing equation. After a disturbance, like a loss of generation, the speed of the machines in different parts of a large power system varies with different oscillations. However, frequency stability is determined by the overall response as evidenced by its mean frequency [29]. This mean frequency conducts to the concept of an aggregated dynamic model, which can estimate the essential characteristics of a synchronously isolated system's frequency response [11], [30]. Considering the inertia constant of the generation units, the aggregated inertia of the system is:

$$H_{\text{sys}} = \frac{\sum_{i=1}^{N} S_{\text{n}i} H_i}{\sum_{i=1}^{N} S_{\text{n}i}} = \frac{E_{k,\text{sys}}}{S_{\text{tot}}} \tag{5}$$

where $S_{\text{n}i}$ is the rated power of generator i [MVA], H_i is the inertia constant of generator i [s], $E_{k,\text{sys}}$ is the system rotational energy [MWs] and S_{tot} is the total rated power of the generators [MVA]. It is possible to derive then the aggregated swing equation for the whole system, given a generation-load imbalance ΔP_{L}:

$$\frac{df}{dt} = \frac{f_0}{2H_{\text{sys}} S_{\text{tot}}} \Delta P_{\text{L}} \tag{6}$$

Three metrics are considered to address the frequency security and stability:

C1) Minimum kinetic energy.

C2) Minimum available synchronous capacity.

C3) Maximum level of System Non-Synchronous Penetration.

These metrics represent different aspects that have impacts on the system inertia and are introduced below.

1) MINIMUM KINETIC ENERGY

The minimum kinetic energy $E_{k,\min}$ needed for a defined admissible value of the *ROCOF* in the system is introduced under the condition:

$$\sum_{i=1}^{N} x_{i,t} H_i S_{\text{n}i} \geq E_{k,\min} \tag{7}$$

where $x_{i,t}$ is a binary variable that represents the i-th generator status (0 = offline, 1 = online) at time t for $i = 1, 2, \ldots, N$.

To define the *ROCOF* withstand capability correctly, the characteristics of an entire synchronous area must be considered. The capability shall be determined based on the analysis of a reference incident for the concerned grid. Such a reference incident could be a system split in a large synchronous area with a significant change of inertia and power imbalance in the resulting subsystems. With regards to smaller synchronous areas with low inertia, the loss of the largest power generating module or HVDC link may define the reference incident. The *ROCOF* withstand capability should ideally be provided as a change in frequency over a defined time period, which filters short-term transients and therefore reflects the actual change in the synchronous grid frequency [31]. Based on results from studies done by the ENTSO-E System Protection & Dynamics Sub Group [9], [32] and better harmonization between the connection codes, the overall system should be stable if the *ROCOF* is cumulatively equal or less to 2 Hz/s. The minimum kinetic energy that should be present in the system is given by:

$$E_{k,\min} \geq \frac{f_0 \Delta P_{\text{L}}}{2\left(\frac{df}{dt}\right)_{\max}} \tag{8}$$

In this paper, the admissible *ROCOF* is 2 Hz/s and a sensitivity analysis on the imbalance is performed, depending on the size of the system. *ROCOF* values higher than 2 Hz/s indicate critical events that, in some cases, can start a chain reaction of adverse events and drive the system to unpredictable system states.

2) MINIMUM AVAILABLE SYNCHRONOUS CAPACITY

In this case, the minimum available synchronous capacity $S_{t,\min}$ is considered to feed a percentage of the total demand capacity. $S_{t,\min}$ is defined as a fraction ψ of the demand capacity $S_{t,\text{load}}$ (the total load apparent power at hour t):

$$S_{t,\min} \geq \psi S_{t,\text{load}} \tag{9a}$$

such that

$$\sum_{i=1}^{N} x_{i,t} S_i \geq S_{t,\min} \tag{9b}$$

In this paper, we consider a sensitivity analysis with different values of the fraction ψ. The synchronous capacity is directly linked to the inertia of the system, improving the frequency stability but affecting the cost for the system.

3) MAXIMUM LEVEL OF SYSTEM NON-SYNCHRONOUS PENETRATION

The System Non-Synchronous Penetration (*SNSP*) ratio ξ_{SNSP} is a dimensionless indicator based on [33] and recently adopted by the Irish TSO [34], defined in [35] as:

$$\xi_{SNSP}(t) = \frac{P_{\text{PEIG}}(t) + P_{\text{import}}(t)}{P_{\text{demand}}(t) + P_{\text{export}}(t)} \tag{10}$$

where $P_{\text{PEIG}}(t)$ is the power generation by PEIG [MW] at time t, $P_{\text{import}}(t)$ is the imported power through HVDC [MW] at time t, $P_{\text{demand}}(t)$ is the power demand [MW] at time t, and

P_{export} represents the exported power through HVDC [MW] at time t.

The *SNSP* index has been selected from a specific set of feasible indicators assessing flexibility requirements for the power system [36] as the most representative of PEIG integration. Recent studies conducted by the Italian TSO have evaluated the average value of the *SNSP* index for the whole Italian power system [37] and for a specific critical section of the Italian power system [38].

This indicator is limited by the maximum value $\xi_{\max}$:

$$\xi_{SNSP} \leq \xi_{\max} \tag{11}$$

The value considered for Ireland was $\xi_{\max} = 0.5$ in [39]. The conclusions of the Irish TSO recommend a restriction on "inertialess penetration" to about 50%, which has been recently extended to 65%, and it is expected to arrive at 75% in the next future [40]. For this purpose, in this paper a sensitivity analysis is considered with $\xi_{\max} = [0.5, 0.65, 0.75]$. These values are considered suitable for small power systems, as values 0.5 and 0.65 have been currently handled in the Irish system and a level of 0.75 has been set as a threshold for a secure operation [41].

C. STRUCTURE OF THE PROPOSED METHOD

Starting from the hourly market simulations results in the considered scenarios at year 2030, the online thermal capacity needed is identified based on fixed and variable costs and minimum stable power of the generating units. If the available thermal capacity does not satisfy the maximum admissible constraint, consecutive iterations are carried out comparing the remaining available thermal units in terms of economic efficiency (merit order) and technical characteristics (minimum stable power).

Once the hourly annual thermal production profiles are defined, input data are modified, and market simulations are repeated. Fig. 1 shows the flowchart of the methodology.

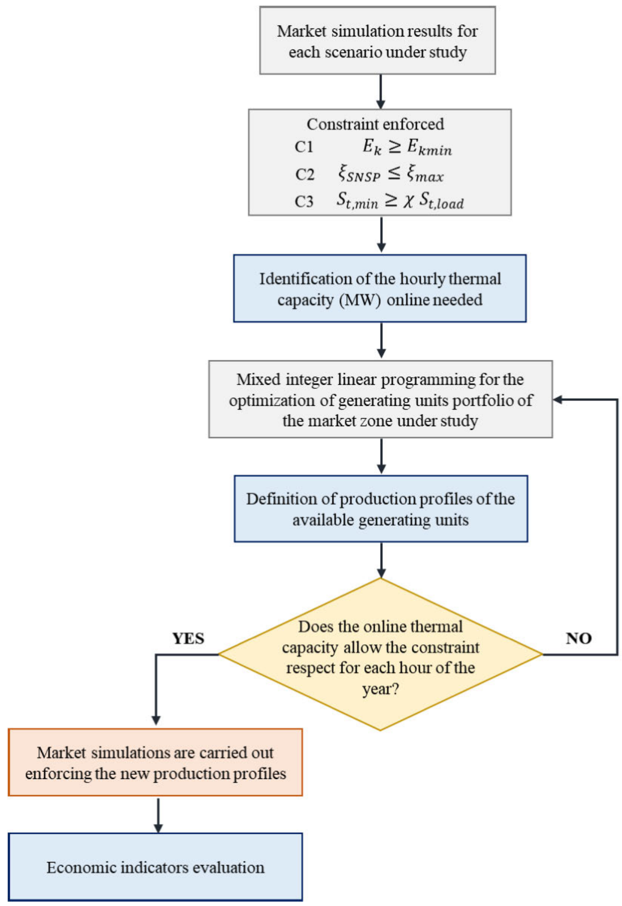

FIGURE 1. Flowchart of the proposed approach with details on how to set the frequency stability constraints.

III. METHODOLOGY FOR THE TECHNICAL-ECONOMIC COMPROMISE SELECTION

The methodology developed in this paper follows the workflow depicted in Fig. 2. The base case has no inertia constraints implemented. The three constraints described in the previous paragraphs are implemented in the market optimization tool, which gives different results in terms of hourly power plants unit commitment to respect the imposed constraints. The results are then compared in a technical-economic perspective, considering the frequency stability performance of the system and the associated costs. The frequency stability of the system is assessed for each hour, with a dynamic simulation, considering the hourly worst-case under frequency contingency. A "single-bus frequency model" has been developed, using MATLAB and Simulink, to study primary system-frequency dynamics during the initial post-contingency timeframe. The aggregate model is formed by: ① System inertia; ② Equivalent traditional power plant transfer function with a pole and a zero; ③ Primary frequency control model; and ④ Frequency-dependent loads. More details on the developed aggregate model can be found in [30].

The performance of the frequency response is assessed in terms of the following indicators:

i initial *ROCOF*, and
ii maximum transient frequency deviation with respect to the rated frequency, denoted as Δf_{nadir}.

The economic outcomes from the market simulations are evaluated in terms of the following indicators, defined in [27]:

a. socio-economic welfare (*SEW*),
b. cost of CO_2 emissions, and
c. cost of fuel.

In this context, a decision maker has to take one single solution between the different alternatives proposed and can do this by experience. Nevertheless, when dealing with a large set of suitable solutions, a method to rank the alternatives can be very useful, falling in the context of multiple-criteria decision analysis (MCDA). Therefore, the results are compared and analysed to find non-dominance between the different alternatives, using the Pareto theory. In practice, for a multi-objective optimization problem, a solution u_1 is said to dominate a solution u_2 if both the next conditions are true:

a) The solution u_1 is not worse than u_2 in all objectives.

b) The solution u_1 is strictly better than u_2 in at least one objective.

After obtaining the Pareto front of the optimization problem, the decision maker needs to select one solution, which will satisfy the different goals to some extent. Such a solution is called best compromise solution.

The selection of the best compromise in terms of technical and economic values is made using a MCDA tool. In MCDA, each criterion is associated to a weight that reflects its relative importance to the decision. The selection of the weights can be judgmental, reflecting the subjective assessment of experts [42]. The literature offers some tools to assist the decision-making process, with different ways to reduce the impact of the personal judgment of the decision maker. The simple weighted sum is exposed to the uncertainties of the opinions of the decision makers. The Analytic Hierarchy Process uses the 9-point scale defined by Saaty [43] to express the relative preferences between pairs of criteria, and applies a consistency criterion to ensure that the preferences have been expressed in a consistent way. The Ordered Weighted Averaging [44] orders the weights based on their relative importance, and uses a transformation function to modify the weighted values of the criteria and obtain a multi-criteria combination procedure guided by a single parameter. The TOPSIS method evaluates the criteria based on their distance to reference (ideal) points [45], [46]. Other methods that compare pairs of weights are ELECTRE [47] and PROMETHEE [48].

The selection of the weights is a crucial point for any multi-criteria assessment. For example, the weighting of criteria to be assessed in extreme situations, such as blackouts, together with other objectives assessed in normal situations, would be a critical issue, because of the excessive difference between these situations. However, this is not the case of the criteria considered in this paper. The TOPSIS tool is used the application shown below, because the criteria are compared among them based on their relative closeness to the ideal solution, thus introducing a quantitative reference that reduces the impact of subjective judgement.

A. CRITERIA FOR MCDA

Five criteria to be minimized are considered:

a) $ROCOF_{95\%}$, the value of $ROCOF$ occurring in 95% of the cases with violations compared to a predefined system $ROCOF$ threshold;
b) $\Delta f_{nadir95\%} = f_0 - f_{nadir95\%}$, the difference between the nominal frequency and the value of frequency nadir occurring in 95% of the cases with violations compared to a predefined system frequency nadir threshold;
c) χ_{SEW}, the ratio between the SEW calculated in the constrained alternative and in the base case;
d) χ_{CO_2}, the ratio between the cost of CO_2 calculated in the constrained alternative and in the base case;
e) χ_{fuel}, the ratio between the cost of fuel calculated in the constrained alternative and in the base case.

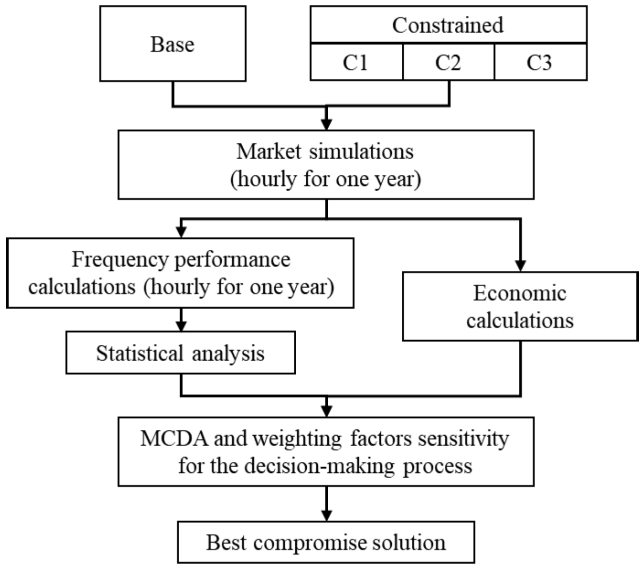

FIGURE 2. Flowchart of the proposed methodology to implement and evaluate the technical and economic performance of the frequency stability constraints in the market simulations.

B. TOPSIS METHOD

The TOPSIS method, based on the concept that the chosen alternative should have the shortest distance from the positive ideal solution and the farthest distance from the negative ideal solution, can identify the best alternative from a finite set of alternatives quickly. The application of TOPSIS [49] is expressed as follows:

1) CONSTRUCT THE NORMALIZED DECISION MATRIX

The normalized decision matrix $\mathbf{R} = \{r_{mz}\}$ is constructed starting from the matrix $\mathbf{D} = \{d_{mz}\}$ of $m= 1, \ldots, M$ alternatives and $z= 1, \ldots, Z$ criteria; for each column $z= 1, \ldots, Z$:

$$r_{mz} = \frac{d_{mz}}{\sqrt{(d_{1z}^2 + \ldots + d_{Mz}^2)}} \tag{12}$$

2) CONSTRUCT THE WEIGHTED NORMALIZED DECISION MATRIX

In the MCDA, the decision maker's weighting factors need to be defined for each criterion, to consider the importance the decision makers can give to different criteria. The weighted normalized decision matrix is constructed using the decision maker's weighting factors λ_z applied to the criteria $z= 1, \ldots, Z$ and the information entropy[2] given by Δ_z:

$$\Delta_z = -k \sum_{m=1}^{M} \frac{d_{mz}}{(d_{1z} + \ldots + d_{Mz})} \ln\left(\frac{d_{mz}}{(d_{1z} + \ldots + d_{Mz})}\right) \tag{13}$$

[2]Given M independent events (i.e., the M alternatives) with probability p_m for $m = 1, \ldots, M$, the Shannon entropy is expressed as $E = -\sum_{m=1}^{M} p_m \ln(p_m)$ and corresponds to the average amount of information received per event [50]. The maximum Shannon entropy $E_{max} = ln(M)$ is obtained when all events have equal probability, that is, $p_m = \frac{1}{M}$. The information entropy measure used in (13) is the normalised Shannon entropy calculated by considering the M alternatives as independent events for the criterion z under analysis.

where $0 \leq \Delta_z \leq 1$ using $k = \frac{1}{\ln M}$. The aggregated weight w_z is computed as:

$$w_z = \frac{\lambda_z \frac{1-\Delta_z}{\sum_{j=1}^{Z}(1-\Delta_j)}}{\sum_{v=1}^{Z} \lambda_v \frac{1-\Delta_v}{\sum_{j=1}^{Z}(1-\Delta_j)}} \tag{14}$$

The weighted normalised decision matrix is given by:

$$\mathbf{V} = \mathbf{R} \cdot \mathbf{W}_{Z\times Z} \tag{15}$$

where $\mathbf{W}_{Z\times Z}$ is the diagonal matrix with the elements w_z on the diagonal.

3) IDENTIFY THE POSITIVE AND NEGATIVE IDEAL SOLUTIONS

The positive and negative ideal solutions of the alternatives are taken from the best and worst elements of the matrix $\mathbf{V}$, respectively:

$$\boldsymbol{a}^+ = \left\{v_1^+, \ldots, v_Z^+\right\}; \boldsymbol{a}^- = \left\{v_1^-, \ldots, v_Z^-\right\} \tag{16}$$

4) DISTANCE OF THE ALTERNATIVES FROM THE IDEAL SOLUTIONS

The distances of each alternative from the positive and negative ideal solutions are given by:

$$\delta_m^+ = \sqrt{\sum_{z=1}^{Z} \left(v_{mz} - v_z^+\right)^2}; \delta_m^- = \sqrt{\sum_{z=1}^{Z} \left(v_{mz} - v_z^-\right)^2} \tag{17}$$

5) CALCULATE THE RELATIVE CLOSENESS TO THE IDEAL SOLUTION

The relative closeness coefficient c_m of each alternative is:

$$c_m = \frac{\delta_m^-}{\delta_m^- + \delta_m^+} \tag{18}$$

6) RANK THE PREFERENCE ORDER

The alternatives are ranked in descending order of c_m. The best solution has the maximum value of c_m.

C. DECISION MAKER'S WEIGHTING FACTORS

To give a broader view on the choice of the weighting factors in the decision-making process, a sensitivity analysis has been implemented. At first, the criteria have been divided into two groups, namely, frequency stability performance criteria (with cardinality σ_f) and cost-based performance criteria (with cardinality σ_c). Then, equal weights have been established for the frequency stability performance criteria ($\lambda_{f,1} = \lambda_{f,2} = \ldots = \lambda_{f,\sigma_f} = 1/\sigma_f$) and for the cost-based performance criteria ($\lambda_{c,1} = \lambda_{c,2} = \ldots = \lambda_{c,\sigma_c} = 1/\sigma_c$).

The parametric analysis has been executed by assuming a coefficient of variation α for the two groups of performance criteria, such that the outcome of the parametric analysis depends only on the coefficient α that satisfies the relation:

$$\alpha \sum_{v=1}^{\sigma_f} \lambda_{f,v} + (1-\alpha) \sum_{q=1}^{\sigma_c} \lambda_{c,q} = 1 \tag{19}$$

TABLE 2. Alternatives analysed with values to evaluate the constraints.

Alternative number	Alternative	Feature	Value
1	Base	No constraints	
2	C1 – Min E_k	Imbalance	500
3	C2 – Min Cap	ψ	0.1
4		ψ	0.3
5		ψ	0.5
6	C3 – *SNSP*	*SNSP*	0.5
7		*SNSP*	0.65
8		*SNSP*	0.75

For $\alpha = 0$ only the cost-based performance criteria are considered, while for $\alpha = 1$ only the frequency stability performance criteria are considered.

IV. CASE STUDY

The Sardinian power system is taken as a real case of interest for testing the proposed methodology with market simulations including the inertia constraint. An overview of the Sardinian generation, demand and transmission system is given in [51]. It consists of an insular power system characterized by a maximum load of 1500 MW and presently connected to the peninsular network by means of two HVDC submarine links: the three terminal Sardinia–Corsica–Peninsula (Centre–North market zone) named SACOI, and the Sardinia–Peninsula (Centre–South market zone) named SAPEI. Both HVDC links can modify active power exchanges depending on the frequency variations of the Sardinia grid, providing frequency power regulation. The Italian TSO's 2018 National Network Development Plan foresees the new submarine HVDC "Tyrrhenian Link" between Sardinia, Sicily and Peninsula. For the DG scenario in the 2030 horizon (characterized by the highest shares of new distributed energy sources, 1.7 GW of PV, 1.4 GW of wind, compared to the current 0.8 GW in PV, 1 GW in wind in 2018), the methodology described in Section II.C has been applied, obtaining a total of 7 use cases analysed, as listed in Table 2. In particular:

- the base case has no inertia constraints implemented;
- the minimum kinetic energy constraint is calculated using an admissible *ROCOF* of 2 Hz/s and an imbalance of 500 MW (the size of the possible reference incident in Sardinia);
- the minimum available synchronous capacity is calculated using the fractions $\psi = [0.1, 0.3, 0.5]$;
- the maximum level of *SNSP* is determined with $\xi_{max} = [0.5, 0.65, 0.75]$.

A. TECHNICAL-ECONOMIC RESULTS AND MCDA

As different constraints are set up, the market simulations provide the different dispatching results, and the hourly kinetic energy is computed. The kinetic energy is assessed

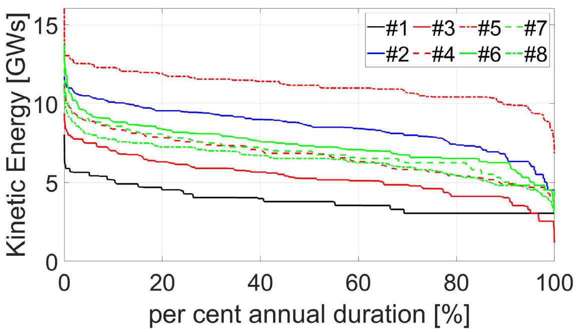

FIGURE 3. Kinetic energy duration curves for the analysed alternatives.

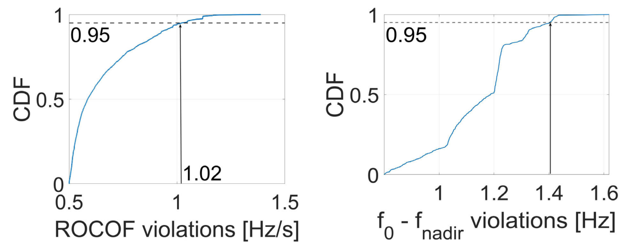

FIGURE 4. Empirical cumulative distribution functions for the *ROCOF* and $f_0 - f_{nadir}$ violations and values observed at least in 95% of the cases.

TABLE 3. Values of each criterion for each alternative.

Alternative number	$ROCOF_{95\%}$	$\Delta f_{nadir95\%}$	χ_{SEW}	χ_{CO_2}	χ_{fuel}
1	1.948	1.429	1.000	1.000	1.000
2	1.020	1.403	1.277	6.530	12.643
3	1.371	1.432	1.137	2.682	5.737
4	1.067	1.325	1.218	6.843	8.811
5	0.808	1.221	1.454	11.987	20.913
6	1.023	1.357	1.306	4.054	13.371
7	1.003	1.391	1.281	3.124	12.699
8	1.159	1.407	1.250	2.633	9.885

considering the number of online synchronous generation units, dispatched each hour of the year by market results. The trend of kinetic energy for the alternatives in Table 2 are reported in Fig. 3, as duration curves expressed in percentage of the year, evaluated using (1). The highest values of kinetic energy are in the alternative #5, where this constraint gives the high number of online synchronous generating units.

The hourly market results are used to feed the aggregated dynamic model described in [30] to evaluate the frequency performance indicators. Dynamic simulations are performed for each hour of the year, selecting the worst-case under-frequency contingency as reference incident (it can be either the largest thermal power plant or the HVDC connection, depending on the operating conditions). The cost-based performance indicators are obtained directly from the market simulator. The values of *ROCOF* and frequency nadir are statistically analysed, to find the performance indicators $ROCOF_{95\%}$ and $f_{nadir95\%}$, occurring in the 95% of the cases with violations, as input for the MCDA, jointly with the economic parameters.

The violations have the following alarm thresholds: a) 0.5 Hz/s for the *ROCOF*; b) 49.2 Hz for the frequency nadir. Values higher than 0.5 Hz/s and 49.2 Hz are based on studies performed and published by ENTSO-E [32] as standard for protection settings and as a first alarm threshold for relevant imbalances in the power system. The empirical cumulative distribution functions of the violations and the values taken for 95% probability are depicted in Fig. 4, for the alternative #2. *ROCOF* and $f_0 - f_{nadir}$ violations observed at least in 95% of the cases are considered as suitable estimates for the MCDA.

Table 3 shows the values of each criterion for each alternative. Overall, taking the alternatives as solution points, all the points indicated correspond to non-dominated solutions and belong to the Pareto front, as any solution of this set represents a balance between objectives.

It can be observed that the five criteria correspond to conflicting objectives, as having good frequency performance implies high inertia and a high number of dispatched synchronous generators, and consequently higher costs for the system. After obtaining the Pareto front of the problem, the decision maker is interested in selecting the best compromise solution. To decide which solution could be more effective, the TOPSIS method has been applied by using the following entries: $\lambda_1 = \lambda_2 = \frac{1}{2}$, $\lambda_3 = \lambda_4 = \lambda_5 = \frac{1}{3}$, and $\alpha = 0.5$. The normalized decision matrix $\mathbf{N}$ is shown in Table 4.

The best compromise solution is given in Table 5, with the complete ranking of all options.

The higher variation in cost savings compared with the changes in the frequency performance criteria leads the best solution to the alternative #1 (base case), with a value of $c_m = 0.91$. The base case is the solution currently planned by the Italian TSO. It is important to observe that in the analysed scenario at 2030 horizon, the base case presents already some synchronous generators online (for around 2000 hours out of the year) even without frequency constraints, and this analysis demonstrates that they are enough to guarantee the frequency stability in a technical economic view. The base case is directly followed by the alternatives #3 and #8, with c_m respectively equal to 0.81 and 0.74. Is it noticeable that the alternatives #3 and #8 correspond to lower values of thermal generation dispatched. Nevertheless, giving more relevance to the frequency stability criterion, the best solution moves away from the base case, as shown in the next paragraph.

B. PARAMETRIC ANALYSIS WITH DIFFERENT IMPORTANCE GIVEN TO THE PERFORMANCE CRITERIA

To highlight the importance of the decision maker's weighting factors λ_z in the MCDA, as their variation can change

TABLE 4. **Normalized decision matrix.**

Alternative number	$ROCOF_{95\%}$	$\Delta f_{nadir95\%}$	χ_{SEW}	χ_{CO_2}	χ_{fuel}
1	0.5647	0.3682	0.2836	0.0604	0.0295
2	0.2958	0.3615	0.3622	0.3942	0.3734
3	0.3973	0.3689	0.3226	0.1619	0.1694
4	0.3093	0.3415	0.3455	0.4130	0.2602
5	0.2340	0.3146	0.4123	0.7235	0.6176
6	0.2964	0.3496	0.3704	0.2447	0.3949
7	0.2908	0.3584	0.3633	0.1886	0.3750
8	0.3361	0.3625	0.3546	0.1589	0.2919

TABLE 5. **Closeness coefficients and ranking of all the alternatives.**

Alternative number	1	2	3	4	5	6	7	8
c_m	0.91	0.48	0.81	0.51	0.09	0.61	0.66	0.74
Rank	1st	7th	2nd	6th	8th	5th	4th	3rd

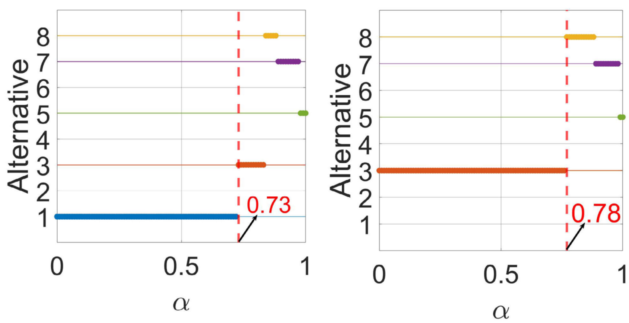

a. With all the alternatives

b. Without the base case

FIGURE 5. **Best alternative for each value for α varying in [0,1] with step 0.01.**

the best solution, a sensitivity analysis has been implemented with α varying between 0 and 1 with step 0.01.

Fig. 5a shows the best alternative selected for each value of α. It is evident that the cost-based performance criteria are dominant until $\alpha = 0.73$, after which the best alternatives are respectively alternative #3, #8, #7 and #5. This means that in the analysed scenario at 2030, the system is planned in a secure way even without frequency constraints, as only high values of α can outline the importance of the frequency stability performance criteria over the costs. If the base case is removed (Fig. 5b), e.g. in the case in which the regulator asks only for inertia constrained alternatives, the best compromise solution is the alternative #3, which corresponds to the lower costs for the system, until $\alpha = 0.78$, after which different alternatives become the best compromise solutions. On these bases, the proposed methodology will be very important and necessary to understand frequency stability in future scenarios at 2050 (which are currently not available, as the long-term development plan covers 10 years) where it is foreseen the complete phase out of coal plants.

V. CONCLUSION

In this paper the impacts of frequency stability security constraints in economic unit commitment have been investigated, in the context of a low inertia power system:

- Multiple frequency constraints have been implemented in a real case study from the Italian TSO andevaluated in a technical economic view, analyzing costs and dynamic performance, with a total of eight different alternatives that can be easily implemented and interpreted for practical scopes.
- The market results have been analysed in terms of frequency stability performing hourly dynamic simulations with an aggregate dynamic model calibrated on the real power system.
- A MCDA process has been outlined to select the best compromise solution, with a parametric analysis on the choice of the decision maker's weighting factors. This method can be easily managed by a decision maker, giving the possibility to use different weights for security and cost importance. Giving more importance in the MCDA to the frequency stability criterion will be necessary to address the growing frequency stability issues in future investigations referring to European scenarios at 2050.

The proposed approach provides the framework for further studies to assess new strategies and technologies to deal with the security requirements in the whole interconnected European grid. ENTSO-E is moving in the same direction, focusing on the implementation of the frequency stability parameters in the cost-benefit analysis [52]. Future works will investigate the admissible limits of the inertia constraints for the system security and their possible interdependencies.

The decision criteria used in this paper have been established by the authors to evaluate future scenarios under the planning and regulatory points of view. The results of the analysis presented in this paper are useful to address policies set up by the regulatory authority, using different weights to represent the importance of security and costs, contributing to the possible introduction of new instruments into the market mechanisms.

REFERENCES

[1] S. Zalzar and E. F. Bompard, "The impacts of an integrated European day-ahead and intraday electricity market on market performance: The Iberian region case," in *Proc. IEEE Milan PowerTech*, Milan, Italy, Jun. 2019, pp. 1–6.
[2] *Renewable Energy, Moving Towards a Low Carbon Economy*, Eur. Commission, Brussels, Belgium, 2018.
[3] *TYNDP 2018 Scenario Report*, ENTSO-E, Brussels, Belgium, Oct. 2018.
[4] B. A. Osbouei, G. A. Taylor, O. Bronckart, J. Maricq, and M. Bradley, "Impact of inertia distribution on power system stability and operation," in *Proc. IEEE Milan PowerTech*, Milan, Italy, Jun. 2019, pp. 1–6.
[5] A. Ulbig, T. S. Borsche, and G. Andersson, "Impact of low rotational inertia on power system stability and operation," *Int. Fed. Autom. Control*, vol. 47, no. 3, pp. 7290–7297, 2014.
[6] E. Ela, V. Gevorgian, A. Tuohy, B. Kirby, M. Milligan, and M. O'Malley, "Market designs for the primary frequency response ancillary service—Part I: Motivation and design," *IEEE Trans. Power Syst.*, vol. 29, no. 1, pp. 421–431, Jan. 2014.

[7] W. Li, P. Du, and N. Lu, "PFR ancillary service in low-inertia power system," *IET Gener., Transmiss. Distrib.*, vol. 14, no. 5, pp. 920–930, Mar. 2020.
[8] T. Xu, W. Jang, and T. Overbye, "Commitment of fast-responding storage devices to mimic inertia for the enhancement of primary frequency response," *IEEE Trans. Power Syst.*, vol. 33, no. 2, pp. 1219–1230, Mar. 2018.
[9] *Frequency Stability Evaluation Criteria for the Synchronous Zone of Continental Europe*, ENTSO-E WG SPD, Brussels, Belgium, Mar. 2016.
[10] H. Gu, R. Yan, and T. K. Saha, "Minimum synchronous inertia requirement of renewable power systems," *IEEE Trans. Power Syst.*, vol. 33, no. 2, pp. 1533–1543, Mar. 2018.
[11] P. Daly, D. Flynn, and N. Cunniffe, "Inertia considerations within unit commitment and economic dispatch for systems with high non-synchronous penetrations," in *Proc. IEEE Eindhoven PowerTech*, Jun. 2015, pp. 1–6.
[12] S. Püschel-Løvengreen and P. Mancarella, "Frequency response constrained economic dispatch with consideration of generation contingency size," in *Proc. Power Syst. Comput. Conf. (PSCC)*, Dublin, Ireland, Jun. 2018, pp. 1–7.
[13] National Grid, London, U.K. (Jun. 2017). *System Needs and Product Strategy*. Accessed: May 18, 2020. [Online]. Available: https://www.nationalgrideso.com/document/84261/download
[14] National Grid, London, U.K. (Feb. 2019). *Future of Frequency Response—Industry Update*. Accessed: May 18, 2020. [Online]. Available: https://www.nationalgrideso.com/document/138861/download
[15] V. Trovato, A. Bialecki, and A. Dallagi, "Unit commitment with inertia-dependent and multispeed allocation of frequency response services," *IEEE Trans. Power Syst.*, vol. 34, no. 2, pp. 1537–1548, Mar. 2019.
[16] L. Badesa, F. Teng, and G. Strbac, "Simultaneous scheduling of multiple frequency services in stochastic unit commitment," *IEEE Trans. Power Syst.*, vol. 34, no. 5, pp. 3858–3868, Sep. 2019.
[17] L. Badesa, F. Teng, and G. Strbac, "Economic value of inertia in low-carbon power systems," in *Proc. IEEE PES Innov. Smart Grid Technol. Conf. Eur. (ISGT-Europe)*, Torin, Italy, Sep. 2017, pp. 1–6.
[18] M. Brito, E. Gil, and I. Calle, "Unit commitment with primary frequency control requirements for low-inertia systems," in *Proc. IEEE Power Energy Soc. Gen. Meeting (PESGM)*, Portland, OR, USA, Aug. 2018, pp. 1–5.
[19] N. Nguyen, V. Johnson, and J. Mitra, "Environmental-economic dispatch of power system in the presence of wind generation," in *Proc. North Amer. Power Symp. (NAPS)*, Charlotte, NC, USA, Oct. 2015, pp. 1–6.
[20] I. J. Raglend, S. Veeravalli, K. Sailaja, B. Sudheera, and D. P. Kothari, "Comparison of AI techniques to solve combined economic emission dispatch problem with line flow constraints," *Int. J. Electr. Power Energy Syst.*, vol. 32, no. 6, pp. 592–598, Jul. 2010.
[21] C.-M. Huang and Y.-C. Huang, "A novel approach to real-time economic emission power dispatch," *IEEE Trans. Power Syst.*, vol. 18, no. 1, pp. 288–294, Feb. 2003.
[22] H. Ahmadi and H. Ghasemi, "Security-constrained unit commitment with linearized system frequency limit constraints," *IEEE Trans. Power Syst.*, vol. 29, no. 4, pp. 1536–1545, Jul. 2014.
[23] F. Teng, V. Trovato, and G. Strbac, "Stochastic scheduling with inertia-dependent fast frequency response requirements," *IEEE Trans. Power Syst.*, vol. 31, no. 2, pp. 1557–1566, Mar. 2016.
[24] Y. Wen, W. Li, G. Huang, and X. Liu, "Frequency dynamics constrained unit commitment with battery energy storage," *IEEE Trans. Power Syst.*, vol. 31, no. 6, pp. 5115–5125, Nov. 2016.
[25] O. Bertoldi and A. Rivoiro, "Fast multiarea economic dispatching for planning applications by accounting for interchange constraints and transmission losses," in *Proc. 12th PSCC*, Dresden, Germany, Aug. 1996, pp. 1–7.
[26] B. Cova *et al.*, "Market integration in Europe: A market simulator taking into account different market zones and the increasing penetration of RES generation," in *Proc. CIGRE Gen. Session*, Paris, France, Aug. 2012, pp. 1–9, Paper C5-101.
[27] *Guideline for Cost Benefit Analysis of Grid Development Process*, ENTSO-E, Brussels, Belgium, 2018.
[28] E. M. Carlini *et al.*, "Impact of CO_2 reduction targets on transmission capacity expansion dictated by the power market clearing: Application to the Italian and French systems," in *Proc. CIGRE*, 2010, pp. 1–9, Paper C5-302.
[29] P. Kundur, *Power System Stability and Control*. New York, NY, USA: McGraw-Hill, 1994.
[30] C. Mosca *et al.*, "Mitigation of frequency stability issues in low inertia power systems using synchronous compensators and battery energy storage systems," *IET Gener., Transmiss. Distrib.*, vol. 13, no. 17, pp. 3951–3959, Sep. 2019.
[31] S. Temtem and K. Creighton, "Summary of studies on rate of change of frequency events on the all-island system," EirGrid & Soni, Dublin, Ireland, Tech. Rep., Aug. 2012.
[32] *Task Force Code—System Dynamic Issues for the Synchronous Zone of Continental Europe*, ENTSO-E WG SPD, Brussels, Belgium, Apr. 2017.
[33] J. O'Sullivan, A. Rogers, D. Flynn, P. Smith, A. Mullane, and M. O'Malley, "Studying the maximum instantaneous non-synchronous generation in an island system—Frequency stability challenges in Ireland," *IEEE Trans. Power Syst.*, vol. 29, no. 6, pp. 2943–2951, Nov. 2014.
[34] EirGrid. (Aug. 27, 2018). *System Non-Synchronous Penetration. Definition and Formulation, Operational Policy*. [Online]. Available: http://www.eirgridgroup.com/site-files/library/EirGrid/SNSP-Formula-External-Publication.pdf
[35] M. Poncela, A. Purvins, and S. Chondrogiannis, "Pan-European analysis on power system flexibility," *Energies*, vol. 11, no. 7, p. 1765, Jul. 2018.
[36] *Scenario Outlook and Adequacy Forecast*, ENTSO-E, Brussels, Belgium, 2015.
[37] L. Michi, M. Migliori, A. C. Bugliari, B. Aluisio, G. M. Giannuzzi, and E. M. Carlini, "Transmission network expansion planning: Towards enhanced renewable integration," in *Proc. AEIT Int. Annu. Conf.*, Bari, Italy, Oct. 2018, pp. 3–5.
[38] L. Michi *et al.*, "The DC power planning for network flexibility in the multi-area power system," in *Proc. AEIT Int. Annu. Conf. (AEIT)*, Bari, Italy, Sep. 2019, pp. 1–5.
[39] K. Creighton *et al.*, "Increased wind generation in Ireland and Northern Ireland and the impact on rate of change of frequency," in *Proc. 12th Wind Integr. Workshop*, London, U.K., Oct. 2013, pp. 1–6.
[40] *Operational Constraints Update*, EirGrid, SONI, Dublin, Ireland, Jan. 2019.
[41] *Delivering a Secure, Sustainable Electricity System (DS3)*, EirGrid, SONI, Dublin, Ireland, 2014.
[42] M. H. Bazerman, *Judgement in Managerial Decision Making*. Hoboken, NJ, USA: Wiley, 2006.
[43] T. L. Saaty, "How to make a decision: The analytic hierarchy process," *Eur. J. Oper. Res.*, vol. 48, no. 1, pp. 9–26, Sep. 1990.
[44] J. Malczewski, T. Chapman, C. Flegel, D. Walters, D. Shrubsole, and M. A. Healy, "GIS-multicriteria evaluation with ordered weighted averaging (OWA): Case study of developing watershed management strategies," *Environ. Planning A, Economy Space*, vol. 35, no. 10, pp. 1769–1784, Oct. 2003.
[45] C. L. Hwang and K. Yoon, *Multiple Attribute Decision Making. Methods and Applications: A State-of-the-Art Survey*. Berlin, Germany: Springer-Verlag, 1981.
[46] A. Mazza and G. Chicco, "Application of TOPSIS in distribution systems multi-objective optimization," in *Proc. 9th World Energy Syst. Conf.*, Suceava, Romania, Jun. 2012, pp. 625–633.
[47] B. Roy, "Classement et choix en présence de points de vue multiples," (in French), *Revue française d'informatique et de recherche opérationnelle*, vol. 2, no. 8, pp. 57–75, 1968.
[48] J.-P. Brans and B. Mareschal, "Promethee methods," in *Multiple Criteria Decision Analysis: State of the Art Surveys* (International Series in Operations Research & Management Science), vol. 78. New York, NY, USA: Springer, 2005, pp. 163–195.
[49] D. L. Olson, "Comparison of weights in TOPSIS models," *Math. Comput. Model.*, vol. 40, nos. 7–8, pp. 721–727, Oct. 2004.
[50] C. E. Shannon, "A mathematical theory of communication," *Bell Syst. Tech. J.*, vol. 27, no. 3, pp. 379–423, Jul./Oct. 1948.
[51] E. Ghiani, S. Mocci, F. Pilo, and G. Celli, "Increasing the flexible use of hydro pumping storage for maximizing the exploitation of RES in sardinia," in *Proc. 3rd Renew. Power Gener. Conf. (RPG)*, Naples, Italy, Sep. 2014, pp. 1–6.
[52] *3rd ENTSO-E Guideline for Cost Benefit Analysis of Grid Development Projects*, Draft Version, ENTSO-E, Brussels, Belgium, Jan. 2020.

CARMELO MOSCA (Member, IEEE) received the M.Sc. degree (Hons.) in electrical engineering from the Politecnico di Torino, Turin, Italy, where he is currently pursuing the Ph.D. degree in electrical, electronics, and communication engineering. His research interests include power system operation and planning, power system dynamics, and renewable energy integration.

ETTORE BOMPARD (Member, IEEE) received the Ph.D. degree in electrical engineering from the Politecnico di Torino, Turin, Italy. He is currently a Professor of Power Systems with the Department of Energy, Politecnico di Torino, and the Scientific Director of the Energy Security Transition Laboratory, Energy Center, Torino. His research interests include electricity markets analysis and simulation, smart grids design and modeling, power system vulnerability assessment and security management, energy security, science-based support to policy decision making, and data analytics applications to power systems.

GIANFRANCO CHICCO (Fellow, IEEE) received the Ph.D. degree in electrotechnics engineering from the Politecnico di Torino (POLITO), Turin, Italy. He is currently a Full Professor of electrical energy systems at POLITO. His research interests include power system and distribution system analysis and optimization, multi-energy system optimization and planning, electrical load management, data analytics, and artificial intelligence applications to energy systems.

BENEDETTO ALUISIO (Member, IEEE) received the M.Sc. degree (Hons.) in electrical engineering and the Ph.D. degree in electrical and information engineering from the Politecnico di Bari, Italy, in 2014 and 2017, respectively. Since 2017, he has been working with TERNA S.p.A., as an Expert in Planning and Grid Studies. Since 2018, he has been a member of an ENTSO-E Planning Standard Drafting Team and TYNDPs working group. He is currently a member of the Grid Planning and Interconnection of Strategy, Development, and System operation Department.

MICHELA MIGLIORI (Student Member, IEEE) received the M.Sc. degree (Hons.) in electrical engineering from the Sapienza University of Rome, and started the Ph.D. degree in electrical engineering in 2017. Since 2017, she has been working with the Italian Transmission System Operator, the Planning Department. Her research interests include power system planning, operation, and economics of electrical energy systems.

CHIARA VERGINE received the M.Sc. degree in electronic engineering from the Sapienza University of Rome. Since 2003, she has been working with GRTN, dealing with Power System Analysis, Cost Benefit Analysis, National Electricity Grid Development Plan. Since 2019, she has also been working with Terna as a responsible for the Reginal Control Centre of North East Italy. In the past, she was responsible of Grid Connection from 2010 to 2015, and Grid Planning. Her research interests include power system planning, operation, and RES integration in power systems.

PAOLO CUCCIA received the M.Sc. degree in electrical engineering from the Politecnico di Torino, Italy. He has been working with Enel since 1989 and with GRTN since 1999, dealing with control systems and network protection systems. Since 2016, he has also been working with Terna as the Head of Dispatching and Operation North West Italy. His research interests include power system operation, electric system faults analysis, and power system planning.